

# UCLA

## UCLA Previously Published Works

### Title

Small-conductance calcium-activated potassium current modulates the ventricular escape rhythm in normal rabbit hearts

### Permalink

<https://escholarship.org/uc/item/9s37g784>

### Journal

Heart Rhythm, 16(4)

### ISSN

1547-5271

### Authors

Wan, Juyi  
Chen, Mu  
Wang, Zhuo  
[et al.](#)

### Publication Date

2019-04-01

### DOI

10.1016/j.hrthm.2018.10.033

Peer reviewed



Published in final edited form as:

*Heart Rhythm*. 2019 April ; 16(4): 615–623. doi:10.1016/j.hrthm.2018.10.033.

## The Small Conductance Calcium Activated Potassium Current Modulates the Ventricular Escape Rhythm in Normal Rabbit Hearts

Juyi Wan, MD<sup>1,3</sup>, Mu Chen, MD<sup>1,4</sup>, Zhuo Wang, MD<sup>1,5</sup>, Thomas H. Everett IV, PhD, FHR<sup>1</sup>, Michael Rubart-von der Lohe, MD<sup>2</sup>, Changyu Shen, PhD<sup>6</sup>, Zhilin Qu, PhD<sup>7</sup>, James N. Weiss, MD<sup>7</sup>, Penelope A. Boyden, PhD<sup>8</sup>, and Peng-Sheng Chen, MD, FHR<sup>1</sup>

<sup>1</sup>Krannert Institute of Cardiology and Division of Cardiology, Indiana University School of Medicine, Indianapolis, IN;

<sup>2</sup>Department of Medicine and Department of Pediatrics, Indiana University School of Medicine, Indianapolis, IN;

<sup>3</sup>Department of Cardiothoracic Surgery, the Affiliated Hospital of Southwest Medical University, Luzhou, Sichuan Province,

<sup>4</sup>Department of Cardiology, Xinhua Hospital, School of Medicine, Shanghai Jiao Tong University, Shanghai,

<sup>5</sup>Department of Cardiology, Renmin Hospital of Wuhan University, Wuhan, China,

<sup>6</sup>Richard and Susan Smith Center for Outcomes Research in Cardiology, Beth Israel Deaconess Medical Center, Harvard Medical School, Boston, MA,

<sup>7</sup>Departments of Medicine (Cardiology) and Physiology, David Geffen School of Medicine at the University of California, Los Angeles, CA

<sup>8</sup>Department of Pharmacology, Columbia University, New York, NY

### Abstract

**Background:** The apamin-sensitive small-conductance calcium-activated K (SK) current ( $I_{KAS}$ ) modulates automaticity of the sinus node;  $I_{KAS}$  blockade by apamin causes sinus bradycardia.

**Objective:** To test the hypothesis that  $I_{KAS}$  modulates ventricular automaticity.

**Methods:** We tested the effects of apamin (100 nM) on ventricular escape rhythms in Langendorff perfused rabbit ventricles with atrioventricular (AV) block (Protocol 1) and on recorded transmembrane action potential (TMP) of pseudotendons of superfused right ventricular (RV) endocardial preparations (Protocol 2).

---

**Address for Correspondence:** Peng-Sheng Chen, MD, 1800 N. Capitol Ave, E475, Indianapolis, IN 46202, Phone: 317-274-0909, chenpp@iu.edu.

**Publisher's Disclaimer:** This is a PDF file of an unedited manuscript that has been accepted for publication. As a service to our customers we are providing this early version of the manuscript. The manuscript will undergo copyediting, typesetting, and review of the resulting proof before it is published in its final citable form. Please note that during the production process errors may be discovered which could affect the content, and all legal disclaimers that apply to the journal pertain.

Disclosures: none

**Results:** All preparations exhibited spontaneous ventricular escape rhythms. In Protocol 1, apamin decreased the atrial rate from  $186.2 \pm 18.0$  bpm to  $163.8 \pm 18.7$  bpm ( $N=6$ ,  $p=0.006$ ) but accelerated the ventricular escape rate from  $51.5 \pm 10.7$  to  $98.2 \pm 25.4$  bpm ( $p=0.031$ ). Three preparations exhibited bursts of nonsustained ventricular tachycardia (NSVT) and pauses, resulting in repeated burst-termination pattern. In Protocol 2, apamin increased the ventricular escape rate from  $70.2 \pm 13.1$  to  $110.1 \pm 2.2$  bpm ( $p=0.035$ ). Spontaneous phase 4 depolarization was recorded from the pseudotendons in 6 of 10 preparations at baseline and in 3 in the presence of apamin. There were no changes of phase 4 slope ( $18.37 \pm 3.55$  vs.  $18.93 \pm 3.26$  mV/s,  $p=0.231$ ,  $N=3$ ), but the threshold of phase 0 activation (mV) reduced from  $-67.97 \pm 1.53$  to  $-75.26 \pm 0.28$  ( $p=0.034$ ). Addition of JTV-519, a ryanodine receptor 2 (RyR2) stabilizer, in 5 preparations reduced escape rate back to baseline.

**Conclusions:** Contrary to its bradycardic effect in the sinus node,  $I_{KAS}$  blockade by apamin accelerates ventricular automaticity and causes repeated NSVT in normal ventricles. RyR2 blockade reversed the apamin effects on ventricular automaticity.

### Keywords

Automaticity; Calcium clock; Idioventricular rhythm; Purkinje cells; Purkinje fibers; Ryanodine receptor; Ventricular tachycardia

### Introduction

The apamin-sensitive small-conductance calcium-activated K (SK) current ( $I_{KAS}$ ) is richly expressed in the atria and pulmonary veins.<sup>1, 2</sup> In addition to its influences on arrhythmogenesis<sup>3, 4</sup>,  $I_{KAS}$  is also important in modulating the automaticity of various atrial structures.<sup>5, 6</sup> The sinoatrial node (SAN) has all 3 subtypes of SK channels (SK1, SK2 and SK3). Heterozygous SK2-null mice have significantly reduced sinus rate as compared with wild type mice.<sup>5</sup> Apamin, a specific SK channel blocker,<sup>7</sup> prolongs action potentials (APs), slows diastolic depolarization and reduces pacemaker rate in isolated SAN cells and intact tissues.<sup>5, 8</sup> Reduction of  $I_{KAS}$  also reduces the automatic rhythm of the atrioventricular (AV) node and pulmonary veins.<sup>5, 8</sup> Based on these findings, it is possible that suppressing the automatic focus in the pulmonary veins by  $I_{KAS}$  blockers could potentially be useful in arrhythmia control. In comparison, very little information is available on the importance of  $I_{KAS}$  in the ventricular escape rhythm in part because the normal ventricular myocytes express minimal or no  $I_{KAS}$ .<sup>2, 9, 10</sup> In contrast to ventricular myocytes, however, we have found that both SK2 proteins and  $I_{KAS}$  are abundantly present in normal rabbit Purkinje fibers.<sup>11</sup> Due to enhanced depolarization, Purkinje fibers are thought to be sources of automaticity and ventricular arrhythmias.<sup>12, 13, 14</sup> That hypothesis is supported by the discovery that primary idiopathic ventricular fibrillation (VF) in patients with normal ventricles is a syndrome characterized by dominant triggers from the distal Purkinje system.<sup>15</sup> Since the molecular mechanisms underlying Purkinje fiber automaticity remain unclear, it is difficult to develop interventions to prevent these lethal cardiac arrhythmias.<sup>16</sup> Accordingly, the goal of this study was to investigate the role of  $I_{KAS}$  in modulating Purkinje fiber automaticity in normal rabbit hearts.

## Methods

All experimental procedures were approved by the Institutional Animal Care and Use Committee of the Indiana University and the Methodist Research Institute, and were conducted in compliance with the Guide for the Care and Use of Laboratory Animals. A total of 19 adult (5–6 months old) New Zealand white rabbits weighing 3.0–3.44 kg were used in this study.

### Protocol 1: Pseudoelectrocardiogram recording in hearts with atrioventricular block

Nine rabbits were used for this protocol. After heparinization (5 mg/kg), the rabbits were euthanized by intravenous sodium pentobarbitone overdose (160 mg/kg, i.v.). The hearts were quickly removed and Langendorff perfused with Tyrode's solution with the following composition (in mM): 125 NaCl, 24 NaHCO<sub>3</sub>, 1.8 NaH<sub>2</sub>PO<sub>4</sub>, 0.5 MgCl<sub>2</sub>, 1.8 CaCl<sub>2</sub>, 4 KCl and 5.5 glucose. The solution was bubbled with 95% O<sub>2</sub> and 5% CO<sub>2</sub> to maintain a pH of 7.40. The perfusion was maintained by a peristaltic pump with a constant flow rate of 30 mL/min. All chemicals were purchased from Sigma-Aldrich (St. Louis, MO). The right atria were cut open to expose the tricuspid annulus. Radiofrequency AV node ablation was performed to achieve complete AV dissociation. Afterwards the hearts were allowed to beat spontaneously. There were no attempts to pace either the atria or the ventricles because pacing could remodel the intracellular Ca distributions and  $I_{KAS}$  expression.<sup>17, 18</sup> Pseudoelectrocardiogram (pECG) was monitored using 2 electrodes placed on the left atrium (LA) and the right ventricle (RV). pECG was recorded continuously by the interactive software program Axoscope continuously throughout the entire experiment. The stabilization period lasted an average of 9.2±1.4 min. The ventricular escape rate at the end of that period was < 100 bpm (RR interval > 600 ms). In the experimental group (N=6), we first recorded 10 min of pECG at baseline. We then added 100 nM apamin into the perfusate and the pECG was continuously recorded for another 30 min. In the control group (N=3), we continuously recorded 50 min of pECG without adding apamin.

### Protocol 2: Transmembrane potential recording in pseudotendons

The hearts were removed and Langendorff perfused as in Protocol 1. After stable spontaneous rhythm was observed for at least 5-min, the RV anterior wall was cut open. A RV flap was then created by cutting the anterior end of RV from the base to the apex along the right side of left anterior descending coronary artery. The pseudotendons were quickly dissected between the free walls and the root of the papillary muscle of the tricuspid valve. Pseudotendons with free running Purkinje fibers were then placed in a Sylgard-coated chamber superfused with Tyrode's solution at 37.0 ± 0.5 °C. The tissue was fixed by stainless steel pins at both ends to minimize motion. Transmembrane potentials (TMPs) were recorded by standard capillary glass microelectrodes drawn from borosilicate thin wall with filament glass (GC150TF-10, Warner Instrument Corp, Hamden, CT) filled with 3 M KCl with a tip resistance ≈ 20 MΩ. The microelectrode was mounted in the micromanipulators and connected by an Ag/AgCl holder to a high-input impedance amplification system. Under microscopic guidance, the tip of microelectrode was inserted into the pseudotendon at its junction with the endocardium to record from the Purkinje fibers. We also recorded from subendocardial myocytes for comparison. An interactive

software program Axoscope provided the data acquisition and AP parameter measurements. After 5 min of baseline recording, 100 nM apamin was added into the superfusate and the membrane potential was continuously recorded for 15 min. In 5 preparations, 1  $\mu$ M JTV-519, a ryanodine receptor 2 (RyR2) stabilizer,<sup>19</sup> was subsequently added into the solution in the continuous presences of apamin. Recordings continued for at least 10 min afterwards.

### Statistics and data analysis

All values are expressed as mean  $\pm$  SEM. Paired Student's t-test was used to compare the variables before and after the agent administration from the same rabbits. Nonparametric signed rank test was used when the data are not normally distributed. Unpaired t test was used to compare the differences of delta escape rate between male and female. Friedman test was used to compare differences among three groups when the data are not normally distributed. Statistical significance was defined as P < 0.05.

## Results

### Protocol-1: Pseudo ECG recording in AV block models

All preparations exhibited a stable ventricular automatic rhythm after AV block. Two types of pECG changes were noted after adding apamin to the perfusate in the experimental group (N=6). The first type occurred in all hearts and was characterized by a gradual increase of the ventricular beating rates accompanied with a decrease of the R wave amplitude, probably due to altered pacemaking site that changed the direction of propagation (Figure 1A). This was followed by gradual slowing of the ventricular activity to baseline. Figure 2 summarizes the differential effects of apamin on ventricular escape rhythm in all hearts studied. Figures 2A and 2B shows the PP and RR intervals at baseline and 11 min after apamin, respectively. Apamin lengthened the PP intervals while shortened the RR intervals. Figure 2C shows the effects of apamin on atrial and ventricular rates all hearts studied. Apamin decreased the atrial rate from  $186.2 \pm 18.0$  bpm to  $163.8 \pm 18.7$  bpm (N=6,  $p=0.006$ ) but accelerated the ventricular rate from  $51.5 \pm 10.7$  to  $98.2 \pm 25.4$  bpm ( $p=0.031$ ).

A second type of response was observed in 3 hearts (Figure 1B). It was characterized by bursts of rapid ventricular activation separated by long pauses. Because these tachycardia episodes usually had more than 3 beats and the rate was significantly faster than the escape rhythm, these episodes qualify as nonsustained ventricular tachycardia (NSVT). Within the NSVT episodes, the ventricular rate was initially fast followed by gradual slowing, leading to the termination of tachycardia. After a long pause, the NSVT then spontaneously reoccurred. This burst-termination pattern repeated itself multiple times before the end of the study. Figure 3 shows the transition from first to second patterns of activation in 3 hearts studied. There was a slowing of ventricular escape rate and premature ventricular contractions (PVCs) prior to the first burst of NSVT.

Figure 4 shows the ventricular escape rates (beats per min or bpm) for all hearts over the entire study. In the control preparations (N=3) without apamin, the ventricular escape rates were initially stable ( $66.3 \pm 11.1$  bpm) followed by gradual reduction to  $37.7 \pm 6.7$  bpm

( $p=0.147$ ) over the 50 min observation period (Figure 4A). No arrhythmias were observed. In comparison, the escape ventricular rates became irregular after adding apamin in the experimental group ( $N=6$ , Figure 4B). The irregularities of the heart rate reflect the occurrence of PVCs and NSVT. All hearts showed at least transient rate acceleration. Hearts 5, 7 and 9 showed burst termination pattern with lowest heart rate reaching zero.

### Protocol-2: Transmembrane potential recording in pseudotendons

We attempted to study 22 isolated in vitro RV preparations but only 10 developed stable spontaneous rhythm when superfused with Tyrode's solution with the RR intervals averaging  $778\pm 77$  ms. Figure 5 shows representative membrane potential recordings from a Purkinje fiber in the pseudotendon (A and B) and a ventricular myocyte from the endocardium (C and D). The APs of the Purkinje fibers but not the ventricular myocytes had spontaneous phase 4 depolarization. Purkinje fibers also had longer  $APD_{80}$  ( $215.4\pm 7.3$  ms) than the ventricular myocytes ( $131.4\pm 17.5$  ms,  $p=0.017$ ). Figure 6A and 6B show recordings before and after apamin administration, respectively. Figure 6C shows the overlapping tracings. While apamin did not change the slope of phase 4 depolarization ( $18.37\pm 3.55$  vs.  $18.93\pm 3.26$  mV/s,  $p=0.231$ ), it resulted in a decrease of the threshold of phase 0 activation ( $-67.97\pm 1.53$  to  $-75.26\pm 0.28$  mV,  $p=0.034$ , Figure 6D). However, only the black trace showed gradual phase 4 to phase 0 transition, consistent with automaticity. The red trace showed abrupt transition, consistent with activation by propagated wavefront. These findings suggest that pacemaking site might have shifted after apamin, making it not possible to compare the threshold of activation at the pacemaking sites.

Figure 7A shows the escape rates of all preparations. The rate increased from  $70\pm 13$  bpm immediately before the addition of apamin (red arrows) to  $110\pm 2$  bpm ( $p=0.035$ ) after addition of 100 nM of apamin (blue arrows). Figure 7B shows the ventricular rates of the second group of 5 preparations. The rates were  $80\pm 12$  bpm at baseline,  $116\pm 12$  bpm after apamin and  $52\pm 4$  bpm after JTV-519 ( $p=0.009$ ). Posthoc tests showed that the rates after apamin were higher than those at baseline and JTV-519 ( $p=0.017$  and  $0.015$ , respectively). However, the rates between baseline and JTV-519 were not significantly different ( $p=0.153$ ). There were no differences between male and females in the delta heart rates before and after adding apamin. The delta escape ventricle rates were  $45.3\pm 16.0$  bpm in males ( $n=4$ ) and  $32.8\pm 7.0$  bpm in females ( $n=6$ ,  $p=0.444$ ).

## Discussion

An interesting finding of this study is that apamin, a highly specific  $I_{KAS}$  blocker,<sup>7</sup> has differential effects on atrial and ventricular rhythms. Consistent with previous reports,<sup>5, 6</sup> apamin slows the atrial rate presumably initiated from the SAN. However, apamin accelerated the ventricular escape rhythm from the Purkinje fibers within pseudotendons. These findings may have important implications in the understanding of ventricular escape rhythms and ventricular arrhythmias in patients with normal hearts.

### Ca clock, $I_{KAS}$ and ventricular escape rhythm

In SAN cells, automaticity depends on both membrane and Ca clocks.<sup>20</sup> Among them, the Ca clock relies on spontaneous Ca releases from the sarcoplasmic reticulum via RyR2 that result in inward  $I_{NCX}$  during late diastolic depolarization. That mechanism is nearly the same in delayed afterdepolarization (DAD) where spontaneous Ca releases in the form of a Ca wave leads to the activation of  $I_{NCX}$  to cause depolarization of membrane potential.<sup>21</sup> This Ca clock mechanism is important both in DAD and SAN automaticity.<sup>22</sup> Optical mapping studies in intact canine right atria showed that spontaneous Ca releases from the SAN is responsible for sinus rate acceleration during isoproterenol infusion.<sup>23</sup> Ryanodine with or without concomitant administration of thapsigargin prevented the spontaneous Ca releases and rate acceleration in that model. JTV-519 suppresses spontaneous Ca release events and Ca waves in Purkinje cells from ischemic zones.<sup>24</sup> In the present study, we showed that JTV-519 slowed the ventricular escape rhythm most likely due to inhibition of intracellular Ca recycling in the Purkinje cells of normal rabbit hearts.

### Heterogeneous distribution of $I_{KAS}$ and the mechanisms of ventricular rate control

$I_{KAS}$  is heterogeneously distributed in the ventricles. It is normally not active in ventricular myocytes but is highly important to the repolarization of Purkinje fibers.<sup>11</sup> Hirose et al<sup>25</sup> reported that both normal and ischemic Purkinje fibers have spontaneous sarcoplasmic reticulum Ca release during the diastole. Cyclic diastolic increases in intracellular Ca may activate the SK channels before the AP upstroke occurs, although the open channel may conduct no or very little current at diastolic potentials. Once the membrane potential becomes less negative during the upstroke, the driving force for  $I_{KAS}$  increases and the resulting outward  $I_{KAS}$  opposes the inward  $I_{Na}$ , increasing the threshold. Apamin, which blocks  $I_{KAS}$ , makes it easier for  $I_{Na}$  to depolarize the membrane, i.e., the threshold is lower and the ventricular rate is faster. An additional factor might be the heterogeneous distribution of SK channels. We found that the threshold of phase 0 activation was reduced by apamin while the slope of phase 4 depolarization remains unchanged. However, in those tracings, the pacemaking site has also shifted as the post-apamin tracing did not show a gradual transition from phase 4 to phase 0. These findings could be explained if the expression of  $I_{KAS}$  is heterogeneous in the His-Purkinje system. Apamin unmasks faster pacing sites that had been suppressed by high  $I_{KAS}$  expression leading to a shift in the dominant pacemaker site remote from the microelectrode recording site. Because we are limited by single cell TMP recordings, we cannot determine if other mechanisms are involved in the ventricular rate acceleration.

### Differential effects of apamin on SAN and Purkinje fibers

Because SAN automaticity also depends on the Ca clock mechanism,<sup>20, 23</sup> the differential effects of apamin on SAN and Purkinje fiber require explanation. SAN cells lack significant  $I_{K1}$  and rely on G-protein gated K channels (Kir3 family).<sup>26, 27</sup> It is possible that  $I_{KAS}$  is needed to set the maximum diastolic potential for optimal  $I_{Ca,L}$  activation. In isolated SAN myocytes, apamin was found to depolarize the maximal diastolic potential, reduce the rate of diastolic depolarization, raise the threshold for the AP upstroke and prolong APD.<sup>6</sup> The first factor would tend to shorten SAN cycle length, but the latter three factors predominated to



prolong SAN cycle length. Purkinje cells, on the other hand, repolarize to a more negative maximum diastolic potential and depend on activation of the  $I_{Na}$ , rather than the  $I_{Ca}$ , to generate the AP upstroke. Presumably, these differences account for the different response to apamin. Because apamin caused the site of the dominant pacemaker to shift to a location remote from the microelectrode, we were unable to determine how the maximum diastolic potential, rate of diastolic depolarization, threshold and APD were affected by apamin. More detailed studies will be required to address the electrophysiological factors underlying the different pacemaking responses of SAN and Purkinje fibers to apamin.

### **$I_{KAS}$ and the burst-termination pattern of cardiac arrhythmias**

In the present study we found that  $I_{KAS}$  blockade often lead to intermittent bursts of NSVT but not torsades de pointes ventricular arrhythmias as observed in failing ventricles.<sup>3</sup> The NSVT episodes were preceded by a period of increased PVCs with frequent long-short coupling intervals. These NSVT episodes are very similar to the nonsustained atrial tachycardia observed in atrial-specific Na/Ca exchanger (NCX) knockout mice.<sup>28</sup> The alternating bursts and pauses occur in NCX knockout mice because of cellular Ca accumulation during spontaneous SAN pacemaker activity producing intermittent hyperactivation of SK channels.<sup>6</sup> Hyperactivation of SK channels in the neurons causes afterhyperpolarization and terminates the neuronal activation, causing burst-termination patterns.<sup>29</sup> Similarly, it was proposed that SK channel hyperactivation can terminate the sinus node activation, causing pauses.<sup>6</sup> However,  $I_{KAS}$  hyperactivation cannot explain the NSVT and pauses in the present study because the NSVT was observed after apamin administration. The mechanisms of these burst termination patterns remain unclear.

### **Clinical implications**

Purkinje potentials have been used to guide the ablation of VT and VF in patients both with and without heart diseases.<sup>15, 30–32</sup> While there is growing consensus that the His-Purkinje system is an important source of ventricular arrhythmia,<sup>16</sup> the mechanisms of arrhythmogenesis from the Purkinje fibers remain incompletely understood. We found that  $I_{KAS}$ , a repolarization current normally presents in large quantities in the Purkinje but not ventricular cells,<sup>11</sup> plays an important role in ventricular automaticity.  $I_{KAS}$  blockade accelerates the automatic rhythm and may promote NSVT in hearts with AV block. These findings suggest that  $I_{KAS}$  may be a new target for managing patients with VT/VF originating from the His Purkinje system of normal hearts. Drugs that block  $I_{KAS}$  (such as amiodarone and ondansetron)<sup>33, 34</sup> may be proarrhythmic in the His-Purkinje system while drugs that blocks RyR2 (such as JTV-519) may be antiarrhythmic. It may be clinically important to determine the  $I_{KAS}$  blocking effects of commonly used drugs to fully assess their proarrhythmic potentials.

### **Limitations**

We have attempted to study 10 LV preparations in Protocol 2, but none of them developed stable spontaneous rhythm. Therefore, we have no TMP data from the LV. JTV-519 while having an effect on SR Ca release may have effects on other ionic currents. Whether or not JTV-519's effects on escape rate is exclusively due to its SR Ca release effects is unclear.



## Acknowledgements

This work was supported in part by the National Institutes of Health grants R01 HL139829, R42DA043391, TR0022080, a National Natural Science Foundation of China grant (No. 81670310), a Charles Fisch Cardiovascular Research Award endowed by Dr Suzanne B. Knoebel of the Krannert Institute of Cardiology, a Medtronic-Zipes Endowment and the Indiana University Health-Indiana University School of Medicine Strategic Research Initiative. We thank Nicole Courtney for her assistance.

## References

- Ozgen N, Dun W, Sosunov EA, Anyukhovskiy EP, Hirose M, Duffy HS, Boyden PA, Rosen MR. Early electrical remodeling in rabbit pulmonary vein results from trafficking of intracellular SK2 channels to membrane sites. *Cardiovasc.Res* 2007;75:758–769. [PubMed: 17588552]
- Xu Y, Tuteja D, Zhang Z, et al. Molecular identification and functional roles of a Ca(2+)-activated K<sup>+</sup> channel in human and mouse hearts. *J Biol Chem*. 2003;278:49085–49094. [PubMed: 13679367]
- Chang PC, Hsieh YC, Hsueh CH, Weiss JN, Lin SF, Chen PS. Apamin induces early afterdepolarizations and Torsades de Pointes ventricular arrhythmia from failing rabbit ventricles exhibiting secondary rises in intracellular calcium. *Heart Rhythm*. 2013;10:1516–1524. [PubMed: 23835258]
- Hsieh YC, Chang PC, Hsueh CH, Lee YS, Shen C, Weiss JN, Chen Z, Ai T, Lin SF, Chen PS. Apamin-sensitive potassium current modulates action potential duration restitution and arrhythmogenesis of failing rabbit ventricles. *Circ Arrhythm Electrophysiol*. 2013;6:410–418. [PubMed: 23420832]
- Zhang Q, Timofeyev V, Lu L, Li N, Singapuri A, Long MK, Bond CT, Adelman JP, Chiamvimonvat N. Functional roles of a Ca<sup>2+</sup>-activated K<sup>+</sup> channel in atrioventricular nodes. *Circ Res*. 2008;102:465–471. [PubMed: 18096820]
- Torrente AG, Zhang R, Wang H, Zaini A, Kim B, Yue X, Philipson KD, Goldhaber JI. Contribution of small conductance K<sup>+</sup> channels to sinoatrial node pacemaker activity: insights from atrial-specific Na<sup>+</sup>/Ca<sup>2+</sup> exchange knockout mice. *J Physiol*. 2017;595:3847–3865. [PubMed: 28346695]
- Yu CC, Ai T, Weiss JN, Chen PS. Apamin does not inhibit human cardiac Na<sup>+</sup> current, L-type Ca<sup>2+</sup> current or other major K<sup>+</sup> currents. *PLoS One*. 2014;9:e96691. [PubMed: 24798465]
- Chen WT, Chen YC, Lu YY, Kao YH, Huang JH, Lin YK, Chen SA, Chen YJ. Apamin modulates electrophysiological characteristics of the pulmonary vein and the Sinoatrial Node. *Eur J Clin Invest*. 2013;43:957–963. [PubMed: 23834267]
- Nagy N, Szuts V, Horvath Z, et al. Does small-conductance calcium-activated potassium channel contribute to cardiac repolarization? *J Mol Cell Cardiol*. 2009;47:656–663. [PubMed: 19632238]
- Chua SK, Chang PC, Maruyama M, et al. Small-conductance calcium-activated potassium channel and recurrent ventricular fibrillation in failing rabbit ventricles. *Circ Res*. 2011;108:971–979. [PubMed: 21350217]
- Reher TA, Wang Z, Hsueh CH, et al. Small-Conductance Calcium-Activated Potassium Current in Normal Rabbit Cardiac Purkinje Cells. *J Am Heart Assoc*. 2017;6:e005471. [PubMed: 28550095]
- Mendez C, Mueller WJ, Merideth J, Moe GK. Interaction of transmembrane potentials in canine purkinje fibers and at purkinje fiber-muscle junctions. *Circulation Research*. 1969;24:361–372. [PubMed: 5766516]
- Singer DH, Lazzara R, Hoffman BF. Interrelationship between automaticity and conduction in Purkinje fibers. *Circ Res*. 1967;21:537–558. [PubMed: 6057710]
- Boyden PA, Dun W, Robinson RB. Cardiac Purkinje fibers and arrhythmias; The GK Moe Award Lecture 2015. *Heart Rhythm*. 2016;13:1172–1181. [PubMed: 26775142]
- Haissaguerre M, Shoda M, Jais P, et al. Mapping and ablation of idiopathic ventricular fibrillation. *Circulation*. 2002;106:962–967. [PubMed: 12186801]
- Haissaguerre M, Vigmond E, Stuyvers B, Hocini M, Bernus O. Ventricular arrhythmias and the His-Purkinje system. *Nat Rev Cardiol*. 2016;13:155–166. [PubMed: 26727298]
- Chan Y-H, Tsai W-C, Ko J-S, Yin D, Chang P-C, Rubart M, Weiss JN, Everett T, Lin SF, Chen P-S. Small conductance calcium-activated potassium current is activated during hypokalemia and

- masks short term cardiac memory induced by ventricular pacing. *Circulation*. 2015;132:1377–1386. [PubMed: 26362634]
18. Jeyaraj D, Wan X, Ficker E, Stelzer JE, Deschenes I, Liu H, Wilson LD, Decker KF, Said TH, Jain MK, Rudy Y, Rosenbaum DS. Ionic bases for electrical remodeling of the canine cardiac ventricle. *Am J Physiol Heart Circ Physiol*. 2013;305:H410–419. [PubMed: 23709598]
  19. Sacherer M, Sedej S, Wakula P, et al. JTV519 (K201) Reduces Sarcoplasmic Reticulum Ca(2+) Leak and Improves Diastolic Function in vitro in Ouabain-Induced Cellular Ca(2+) Overload in Murine and Human Non-Failing Myocardium. *Br J Pharmacol*. 2012.
  20. Lakatta EG, Maltsev VA, Vinogradova TM. A coupled system of intracellular Ca2+ clocks and surface membrane voltage clocks controls the timekeeping mechanism of the heart's pacemaker. *Circ Res*. 2010;106:659–673. [PubMed: 20203315]
  21. ter Keurs HE, Boyden PA. Calcium and arrhythmogenesis. *Physiol Rev*. 2007;87:457–506. [PubMed: 17429038]
  22. Joung B, Zhang H, Shinohara T, Maruyama M, Han S, Kim D, Choi EK, On YK, Lin SF, Chen PS. Delayed afterdepolarization in intact canine sinoatrial node as a novel mechanism for atrial arrhythmia. *J Cardiovasc Electrophysiol*. 2011;22:448–454. [PubMed: 21040091]
  23. Joung B, Tang L, Maruyama M, Han S, Chen Z, Stucky M, Jones LR, Fishbein MC, Weiss JN, Chen PS, Lin SF. Intracellular calcium dynamics and acceleration of sinus rhythm by beta-adrenergic stimulation. *Circulation*. 2009;119:788–796. [PubMed: 19188501]
  24. Boyden PA, Dun W, Barbhaiya C, Ter Keurs HE. 2APB- and JTV519(K201)-sensitive micro Ca2+ waves in arrhythmogenic Purkinje cells that survive in infarcted canine heart. *Heart Rhythm*. 2004;1:218–226. [PubMed: 15851156]
  25. Hirose M, Stuyvers BD, Dun W, ter Keurs HE, Boyden PA. Function of Ca(2+) release channels in Purkinje cells that survive in the infarcted canine heart: a mechanism for triggered Purkinje ectopy. *Circ Arrhythm Electrophysiol*. 2008;1:387–395. [PubMed: 19753099]
  26. Irisawa H, Brown HF, Giles W. Cardiac pacemaking in the sinoatrial node. *Physiol Rev*. 1993;73:197–227. [PubMed: 8380502]
  27. Schram G, Pourrier M, Melnyk P, Nattel S. Differential distribution of cardiac ion channel expression as a basis for regional specialization in electrical function. *Circ Res*. 2002;90:939–950. [PubMed: 12016259]
  28. Torrente AG, Zhang R, Zaini A, Giani JF, Kang J, Lamp ST, Philipson KD, Goldhaber JJ. Burst pacemaker activity of the sinoatrial node in sodium-calcium exchanger knockout mice. *Proc Natl Acad Sci U S A*. 2015;112:9769–9774. [PubMed: 26195795]
  29. Grillner S The motor infrastructure: from ion channels to neuronal networks. *Nat Rev Neurosci*. 2003;4:573–586. [PubMed: 12838332]
  30. Nakagawa H, Beckman KJ, McClelland JH, Wang X, Arruda M, Santoro I, Hazlitt HA, Abdalla I, Singh A, Gossinger H. Radiofrequency catheter ablation of idiopathic left ventricular tachycardia guided by a Purkinje potential. *Circulation*. 1993;88:2607–2617. [PubMed: 8252671]
  31. Lopera G, Stevenson WG, Soejima K, Maisel WH, Koplán B, Sapp JL, Satti SD, Epstein LM. Identification and ablation of three types of ventricular tachycardia involving the hispurkinje system in patients with heart disease. *J Cardiovasc Electrophysiol*. 2004;15:52–58. [PubMed: 15028072]
  32. Haissaguerre M, Extramiana F, Hocini M, et al. Mapping and ablation of ventricular fibrillation associated with long-QT and Brugada syndromes. *Circulation*. 2003;108:925–928. [PubMed: 12925452]
  33. Turker I, Yu C-C, Chang P, Chen Z, Sohma Y, Lin S-F, Chen P-S, Ai T. Amiodarone Inhibits Apamin-Sensitive Potassium Currents. *PLoS One*. 2013;8:e70450. [PubMed: 23922993]
  34. Ko JS, Guo S, Hassel J, et al. Ondansetron Blocks Wildtype and p.F503L Variant Small Conductance Calcium Activated Potassium Channels. *Am J Physiol Heart Circ Physiol*. 2018;315:H375–H388. [PubMed: 29677462]

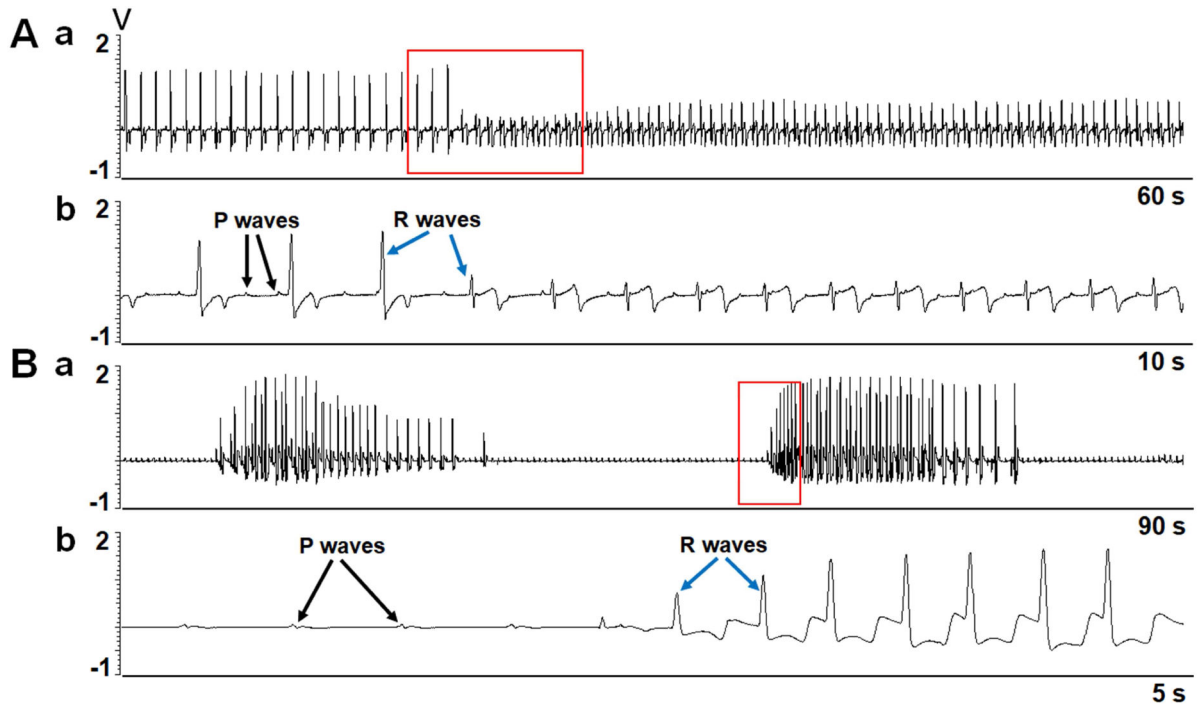


**Figure 1. Effects of apamin on ventricular escape rhythm.**

There are two types of responses to apamin. **A.** acceleration of baseline rate. Subpanel a shows that apamin induced a gradual increase of the ventricular escape rate accompanied by a decrease of the R wave amplitude. The ventricular rate then slowly decelerated to baseline. b: Enlarged from the red box in a, confirming the presence of AV dissociation. **B.** Bursts of NSVT separated by long pauses. Subpanel a shows long pauses and intermittent clusters of ventricular beats after the administration of apamin. Subpanel b shows ECG enlarged from the red box from subpanel a.

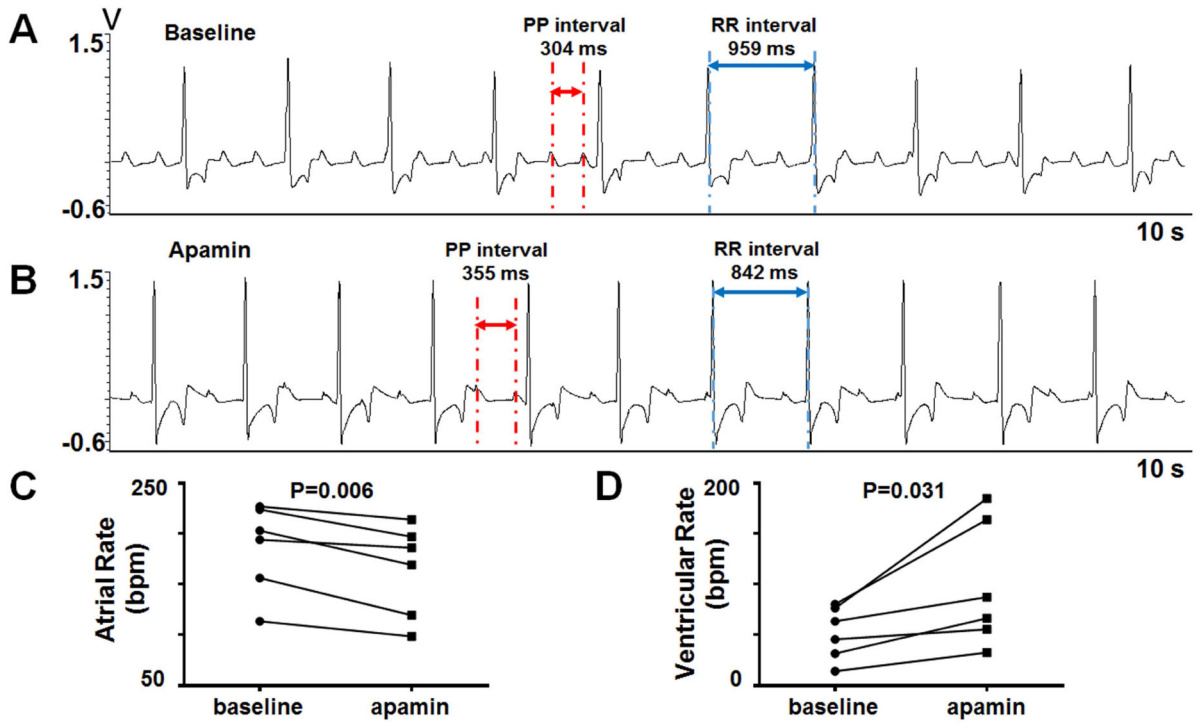


**Figure 2. Differential effects of apamin on atrial and ventricular rhythms.**

**A.** The PP interval and RR intervals at baseline. **B.** Apamin lengthens the PP interval but shortens RR interval in the same heart. **C.** Effects of apamin on atrial rate in all hearts studied. **D.** Effects of apamin on ventricular rate in all hearts studied.

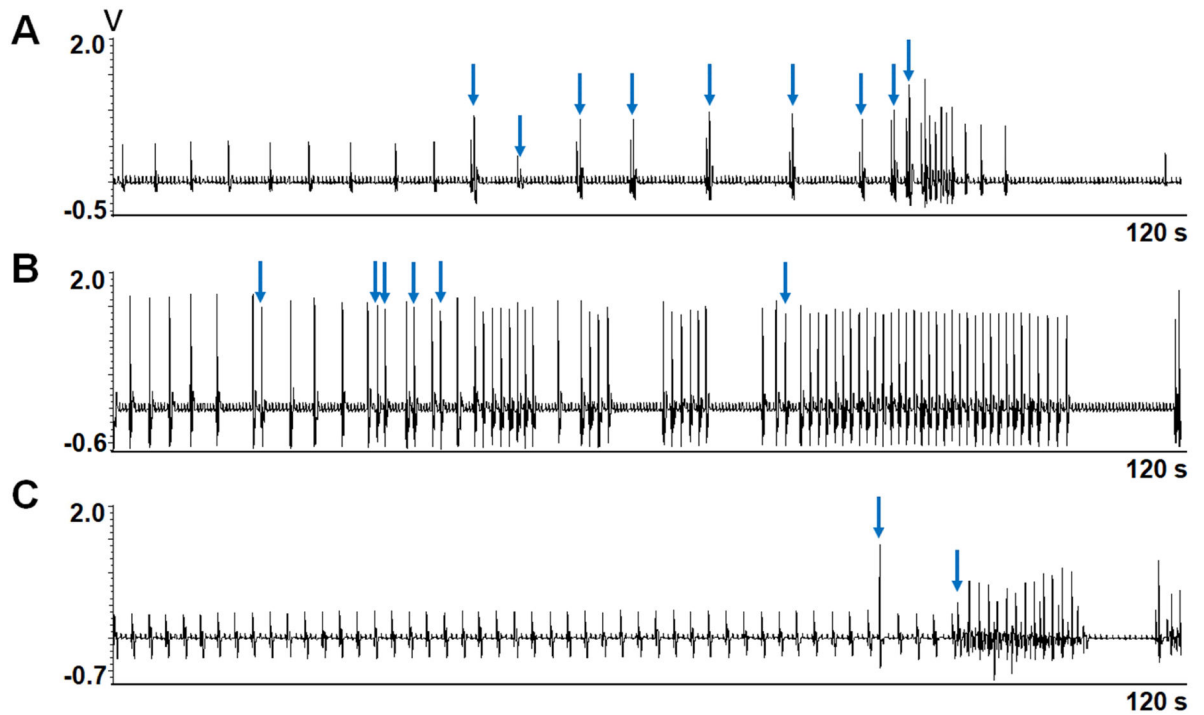


**Figure 3. First episodes of NSVT after addition of apamin.**

A, B and C show the first episodes of the NSVT in 3 different hearts 7.5 min, 11.5 min and 5 min, respectively, after apamin administration. Note the occurrence of premature ventricular contractions (blue arrows) prior to the NSVT episodes.

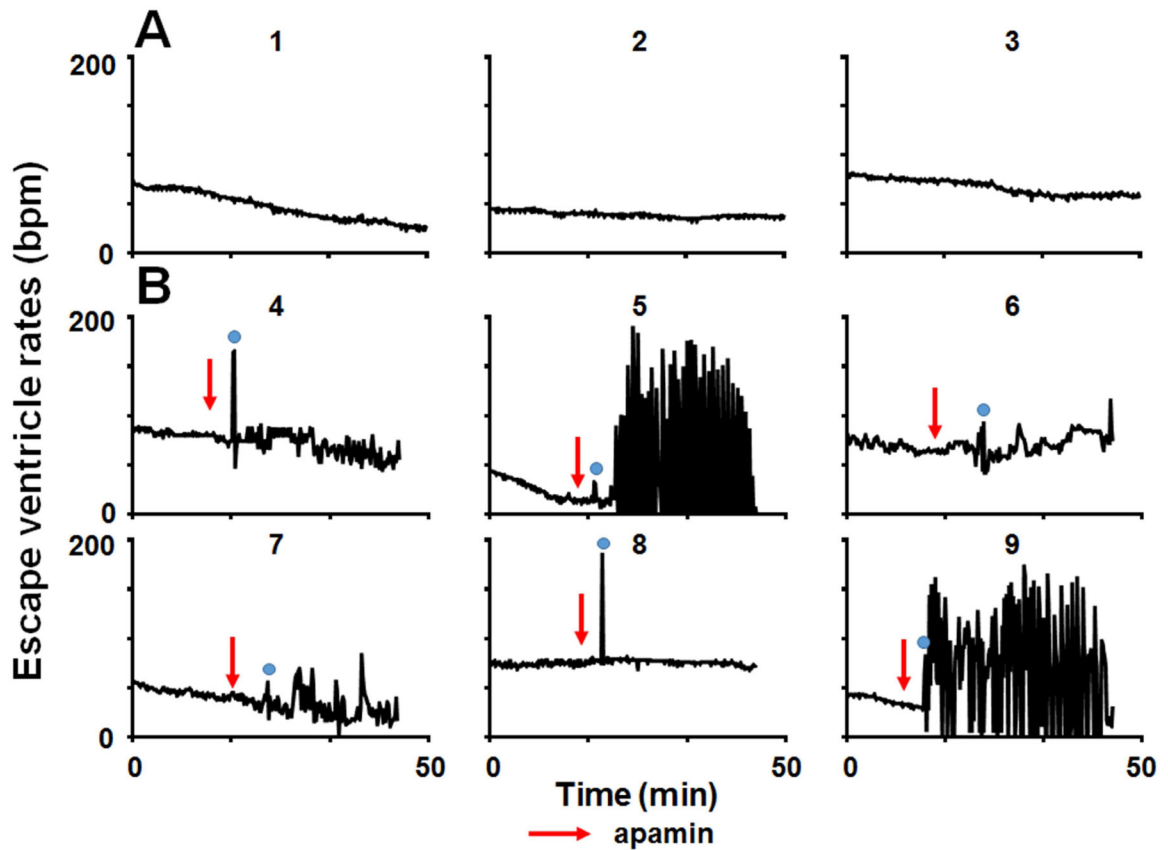


**Figure 4. Apamin accelerates the ventricular escape rhythm in hearts with AV block.**

We calculated the rate in 10-s windows and plotted the results over time for all hearts studied. **A.** The escape ventricular rates in control group showed stable or gradually reduced rates without intermittent acceleration or long pauses. **B.** Apamin increased the escape ventricular rates and induced ventricular arrhythmia in the experimental group. Because of intermittent acceleration and long pauses, the rates varied considerably over time in this group of hearts. Red arrows indicate the time of apamin administration. Blue dots indicate the transient rate acceleration after addition of apamin. NSVT episodes and pauses occurred in hearts 5, 7 and 9. The rates of those hearts have large variations consistent with burst termination pattern.

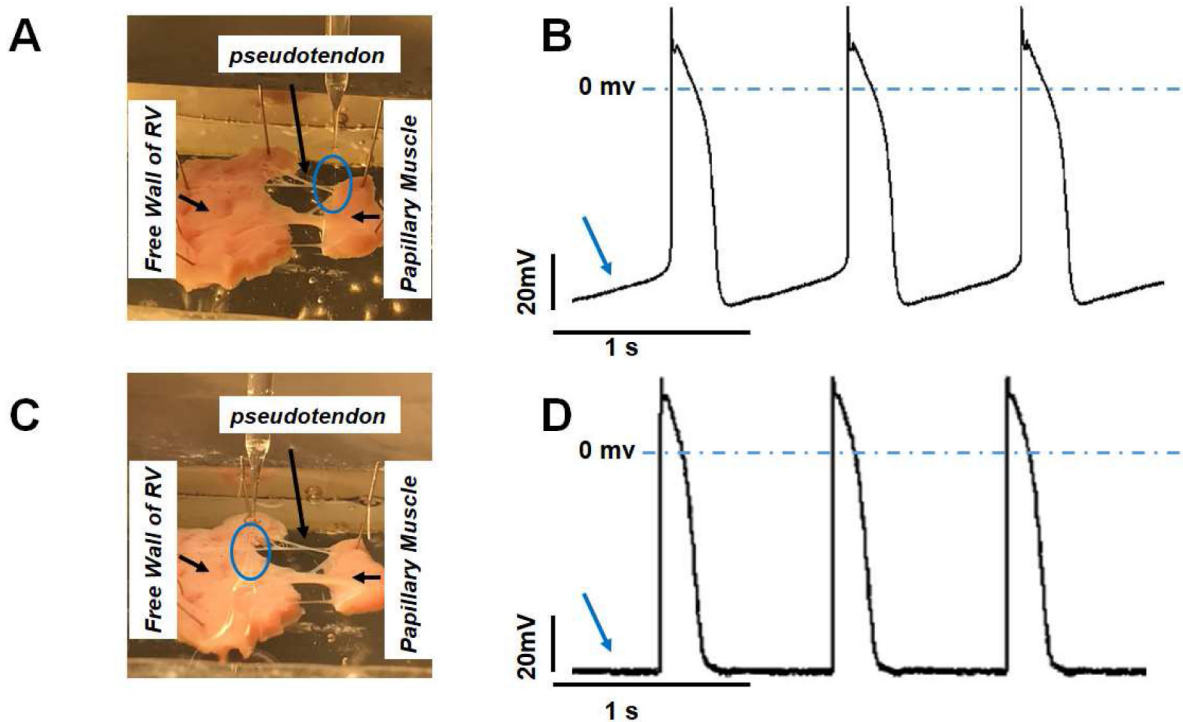


**Figure 5. TMP recording from Purkinje cells and ventricular myocytes.**

**A.** The microelectrode was inserted into a cell at the junction of pseudotendon and ventricular endocardium (blue circle). It is technically difficult to achieve stable impalement in the free running portion of the pseudotendon. **B.** The Purkinje cell action potential (AP), showing spontaneous phase 4 depolarization (arrow). **C.** The microelectrode was placed on the ventricular endocardium, slightly removed from the pseudotendon insertion. **D.** TMP recording of ventricular myocytes showing the absence of spontaneous phase 4 depolarization (arrow). Panels B and D were not recorded simultaneously.



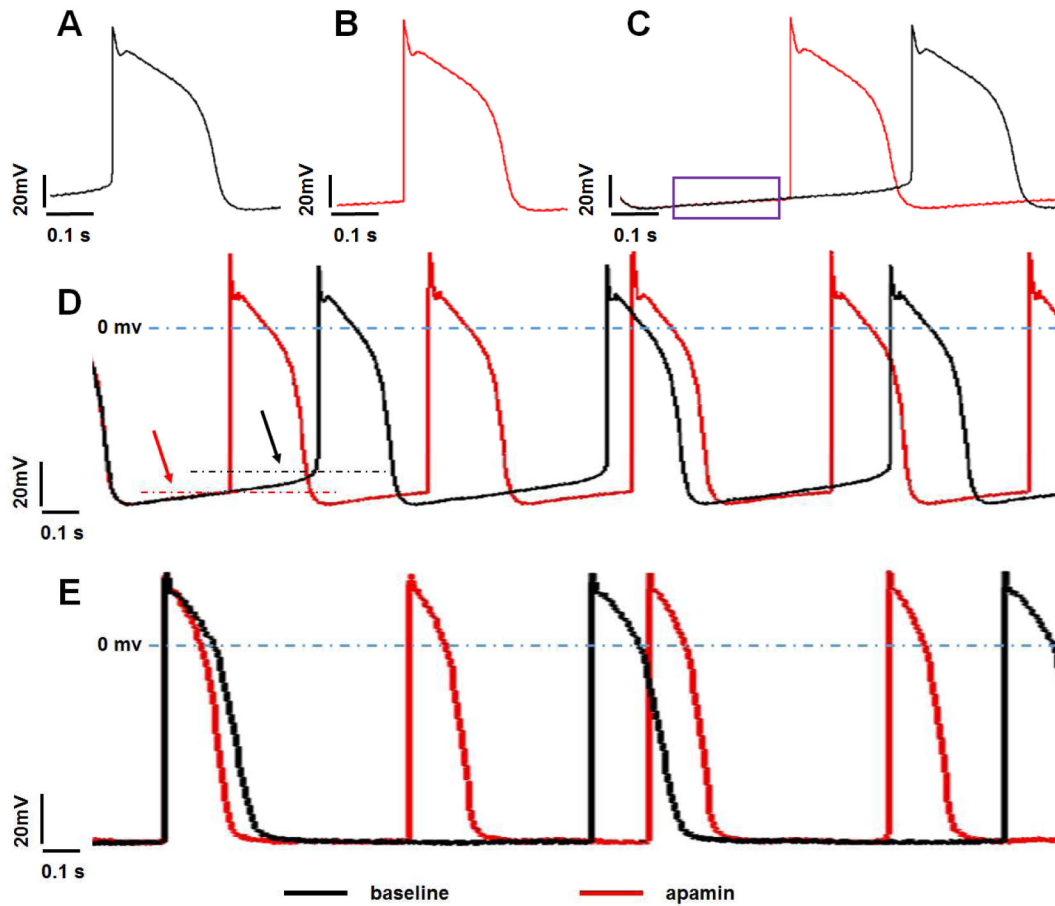


**Figure 6. TMP recordings from Purkinje cells and ventricular myocytes at baseline and after apamin.**

**A.** Purkinje AP at baseline. **B.** Purkinje fiber AP in the presence of apamin. **C.** Overlay of the Purkinje AP recorded at baseline (black) and after apamin (red). Note that the slopes of the phase 4 diastolic depolarization were the same between baseline and after apamin (purple box). **D.** Compared with baseline (black), apamin (red) had lower threshold potential for phase 0 depolarization (dotted line). However, there was abrupt transition between phase 4 and phase 0 in the red trace, suggesting that the pacemaking site has shifted. **E.** Ventricular myocytes AP at baseline and after apamin administration. There are rate related shortening of AP duration. No spontaneous phase 4 depolarization was noted.

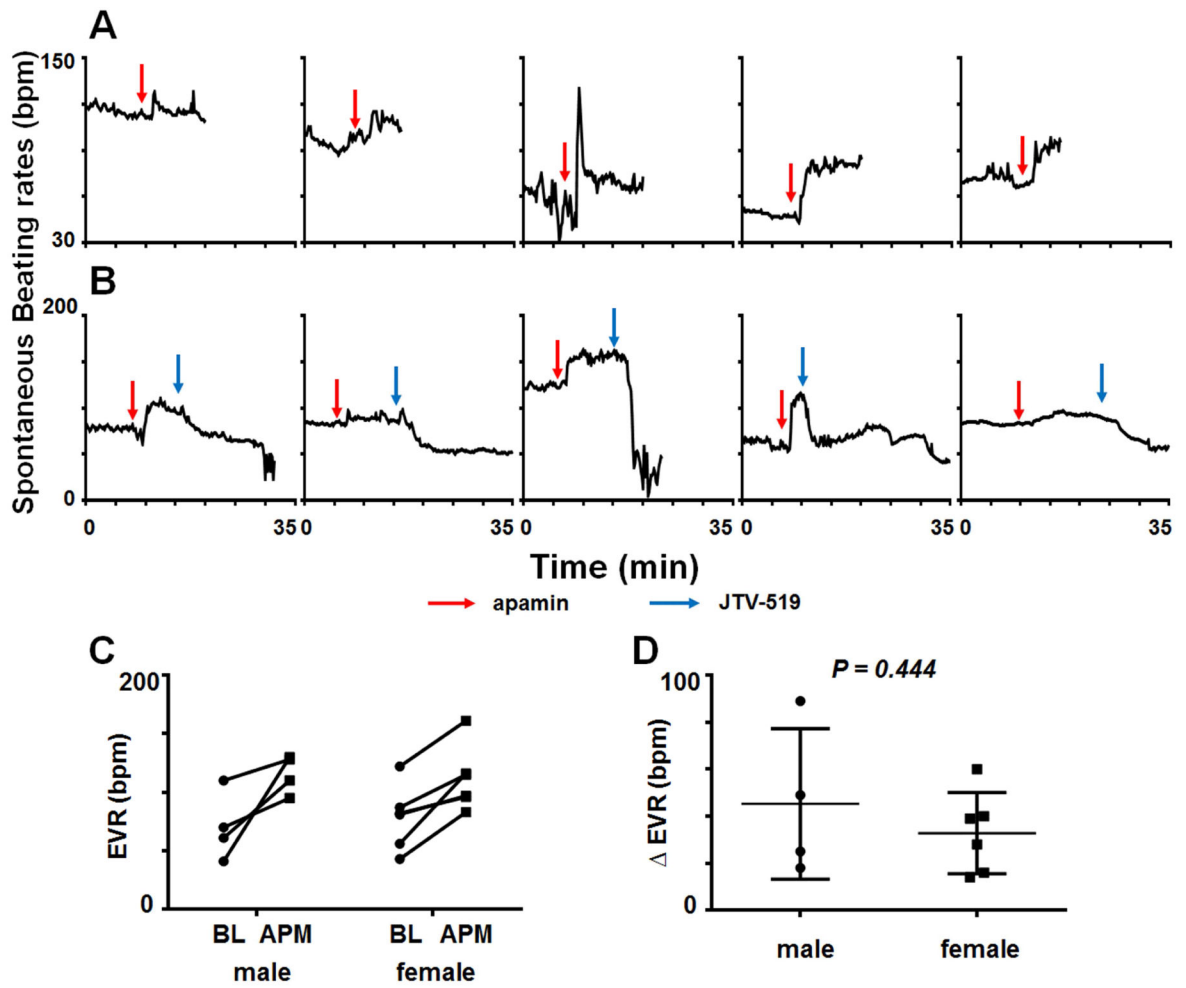


**Figure 7. Apamin increases while JTV-519 decreases phase 4 automaticity of Purkinje cells.**  
**A.** Apamin administration (red arrows) increased the spontaneous AP rates in all 5 Purkinje cells. **B.** In the presence of apamin, JTV-519 administration (blue arrows) decreased the spontaneous AP rates in all 5 Purkinje cells. **C.** The escape ventricle rate (EVR) of baseline (BL) and addition of apamin (APM) in all isolated RV Purkinje fibers. **D.** There were no difference of delta escape ventricle rate after adding apamin between male and female.